Arc Evolution and Variability in Magmatic Porphyry Fertility of the Southern Quesnel Arc, south-central British Columbia (NTS 082E, L, 092H, I, P, 093A, B)

Taylor J. Ledoux *and Craig J.R. Hart
MDRU - Mineral Deposit Research Unit, The University of British Columbia, Vancouver, British Columbia
*tledoux@eoas.ubc.ca

MDRU
MINERAL DEPOSIT RESEARCH UNIT

The Situation

Porphyry Cu deposits are the world's largest repositories of Cu and Mo and are major sources of Au and Ag.

Porphyry Cu deposits are critical contributors to the British Columbia economy with > 290 kt (2018) of Cu concentrate extracted from BC porphyry deposits

BC copper mines generate >$2 billion in annual revenues and contribute to more than half of Canada's Cu production.

The Problem

Demand for copper is anticipated to increase dramatically, particularly with the rise in electrified vehicles and increased infrastructural demands. Society needs more copper – where will it come from? How do we find more porphyry systems?

A Solution

Develop predicative approaches for exploration targeting so that exploration resources and activities are directed to the areas of greater potential success.

The Approach

To determine which magmatic rocks have the greatest potential to generate porphyry copper deposits – we can assess their fertility, their propensity to form an ore deposit.

Porphyry copper deposits form in volcanic arcs and have critical magmatic features such as particular oxidation states, temperature, metal, water, chlorine, and sulphur contents. Arc magmas that have these features are considered to be fertile and more likely to form porphyry copper mineralization.

However, arc rocks are typically altered and the fertility signals can be modified and misleading. But zircon crystals that form within the magma are robust indicators of the magma chemistry. In fact, both the trace element signatures and grain morphology of zircons can indicate many of the fertile attributes.

To use **zircons as porphyry fertility indicators** better, we need to understand their variability across many scales, from within magmatic system to within an evolving arc, to along an arc segment or across an inboard migrating arc. These variations have not been established and is the focus of this research project.

As well, we will develop methods and applications of this technology so that it can be readily utilized by the minerals industry to improve their exploration targeting. We are particularly focusing on the southern Quesnellia arc since its geology has been very well characterized (shout out to Paul Schiarizza and the BCGS) and is clearly productive and prospective.

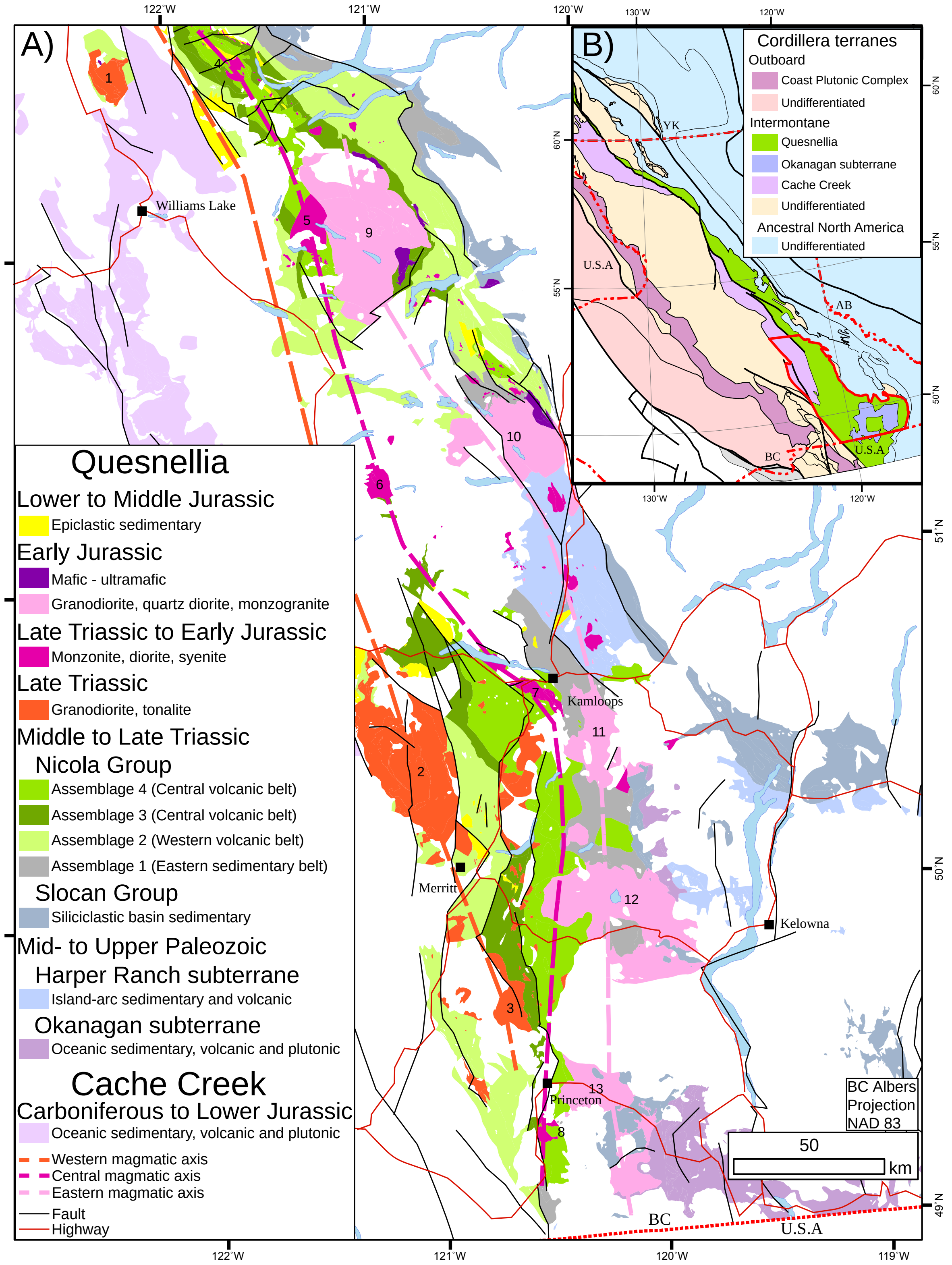

Figure 1. A) Geology of southern Quesnellia and the Cache Creek terrane, south-central British Columbia (modified after Cui et al., 2017). Nicola Group assemblages after Preto (1979), McMillan (1981), Monger (1985) and Schiarizza (2019). Symbols: red dashed line, Western magmatic axis; fuchsia dashed line, Central magmatic axis; pink dashed line, Eastern magmatic axis (modified after Schiarizza (2014). Numbers: 1, Granite Mountain batholith; 2, Guichon Creek batholith; 3, Alice Lake pluton; 4, Mount Polley; 5, Spout Lake pluton; 6, Rayfield River; 7, Iron Mask batholith; 8, Copper Mountain; 9, Takomkane batholith; 10, Thuya batholith; 11, Wild Horse batholith; 12, Pennask batholith; 13, Bromley batholith. **B)** Terranes of British Columbia (modified after Colpron and Nelson, 2020).

Objectives

We will:

1) Describe the evolution of the lithology and tectonic setting of the Quesnellia Arc.

2) Characterize the variability in Late Triassic to Early Jurassic plutonic suites throughout the evolution of the Quesnellia arc.

3) Summarize the methods and sampling that has been completed and outline the future work needed to determine the variability in the Magmatic porphyry fertility of the Quesnellia arc.

Geological Setting

Much of British Columbia is underlain by a series of Mesozoic island-arc and associated accretionary-margin assemblages that were accreted onto the ancestral North American margin.

- Quesnellia is composed of Middle Triassic to Early Jurassic island-arc assemblages and related intrusions of the Nicola and Rossland Group's and the coeval Slocan Group siliciclastic basin (Little, 1960), which are
- Unconformable on the Middle to Upper Paleozoic oceanic Okanagan and island-arc Harper Ranch subterranes (Read and Okulitch, 1977).
- mid-Mesozoic oceanic Cache Creek terrane is faulted against the western margin of Quesnellia (Travers, 1978).
- Eastern Quesnellia is unconformable on the oceanic Slide Mountain terrane and pericratonic Kootenay terrane (Colpron and Price, 1995).

Building the Southern Quesnellia Arc

The lower Mesozoic Quesnellia are primarily Middle to Late Triassic Nicola Group volcanic arc in the west and the coeval Slocan Group siliciclastic basin to the east (Little, 1960; Preto, 1979). Nicola Group forms parallel, linear belts that include four assemblages that are fault bounded in the south and define a regional syncline in the north (Preto 1979; McMillan 1981; Monger, 1985; Schiarizza, 2016).

Construction of the Quesnellia arc started in the Middle Triassic (Anisian) with the deposition of sedimentary and local volcaniclastic and basaltic rocks of **Assemblage 1** (Schiarizza, 2019). As the arc developed in the Late Triassic (early Carnian to early Norian) volcanic sandstones and conglomerates were deposited with calc-alkaline to tholeiitic subaerial basaltic flows and breccias intercalated with limestones and epiclastic sedimentary rocks of **Assemblage 2**.

In the Latest Triassic (Norian) volcanism transitioned from calc-alkaline to high-K, shoshonitic, calc-alkaline to alkaline pyroxene-phyric basaltic flows (Mortimer, 1987) intercalated with lesser volcaniclastic and sedimentary rocks of **Assemblage 3** (Schiarizza, 2019).

In the Latest Triassic (Rhaetian) normal subduction stalled, initiating slab tearing, and higher temperature melting of the metasomatized mantle wedge (Logan and Mihalynuk, 2014) polymict conglomerates with clasts of the alkaline plutonic rocks from the uplifted and eroded arc were deposited, along with lesser volcaniclastics and calc-alkaline and alkaline basaltic and andesitic volcanism of **Assemblage 4**.

Flattening subduction in the Early Jurassic caused the arc to migrate eastward (Parrish and Monger, 1992) resulting in arc volcanism and related sedimentary rocks of the Rossland group in the east, and deposition of arc-derived siliciclastic rocks of the Dragon Mountain Succession and Ashcroft Formation unconformably on the Nicola Group (Schiarizza, 2019). Normal arc subduction beneath Quesnellia ceased shortly after accretion onto Ancestral North America ~186 Ma (Nixon et al., 1993).

Table 1. Characteristics of the Western, Central, and Eastern magmatic axes of the Quesnellia arc. * indicates inferred resources. All other resources are measured and indicated.

	Western magmatic axis	Central magmatic axis	Eastern magmatic axis
Age (Ma)	229–206	207–198.6	202–192.7
Magmatic affinity	Calc-alkaline	Alkaline	Calc-alkaline, high-K calc-alkaline
Predominant rock type	Granodiorite and tonalite	Diorite and monzonite	Granodiorite and quartz diorite
Batholith area (km2)	up to 1300	32–120	up to 1300
Batholith thickness (km)	>6	4	
Average emplacement depth (km)	5	1	4
Major porphyry districts	Highland Valley and Gibraltar	Copper Mountain, Afton-Ajax, and Mount Polley	Brenda and Woodjam
Metal assemblages	Cu-Mo Au	Cu-Au	Cu-Mo & Cu-Au
Historical copper production (Mt)	6.39	1.83	0.28
Current copper resource (Mt)	2.81	4.1	0.79*
Total contained copper (Mt)	9.2	5.93	1.07

* inferred resource

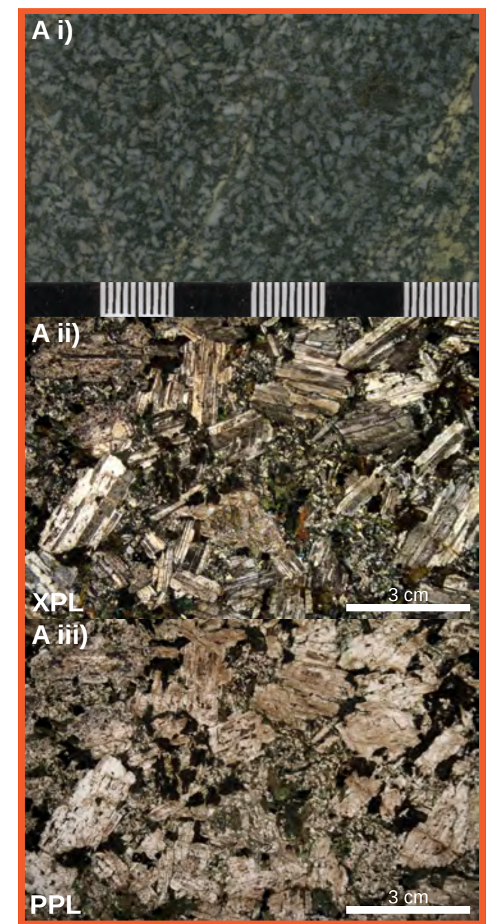

Figure 2. Western Magmatic Axis Petrography. A) Allison lake porphyritic diorite. **i)** scanned rock photographs and transmitted light photomicrographs: **ii)** cross polarized light (XPL) and **iii)** plane polarized light (PPL).

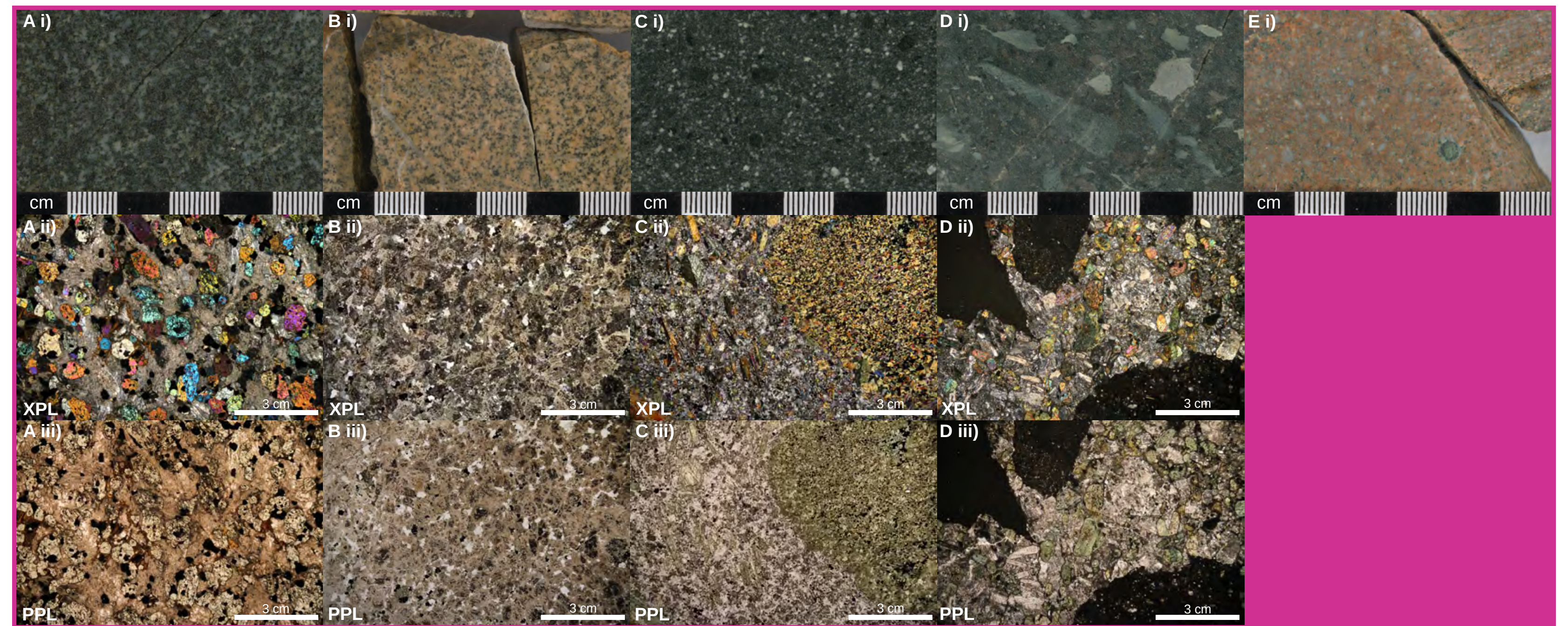

Figure 3. Central Magmatic Axis Petrography. Iron Mask Batholith: **A)** Pothook phase equigranular diorite; **B)** Cherry Creek phase equigranular monzonite; **C)** Sugarloaf phase porphyritic diorite; **D)** Hybrid phase xenolith-rich diorite. Copper Mountain Intrusive Complex: **E)** Lost Horse equigranular monzonite. **i)** scanned rock photographs and transmitted light photomicrographs: **ii)** cross polarized light (XPL) and **iii)** plane polarized light (PPL).

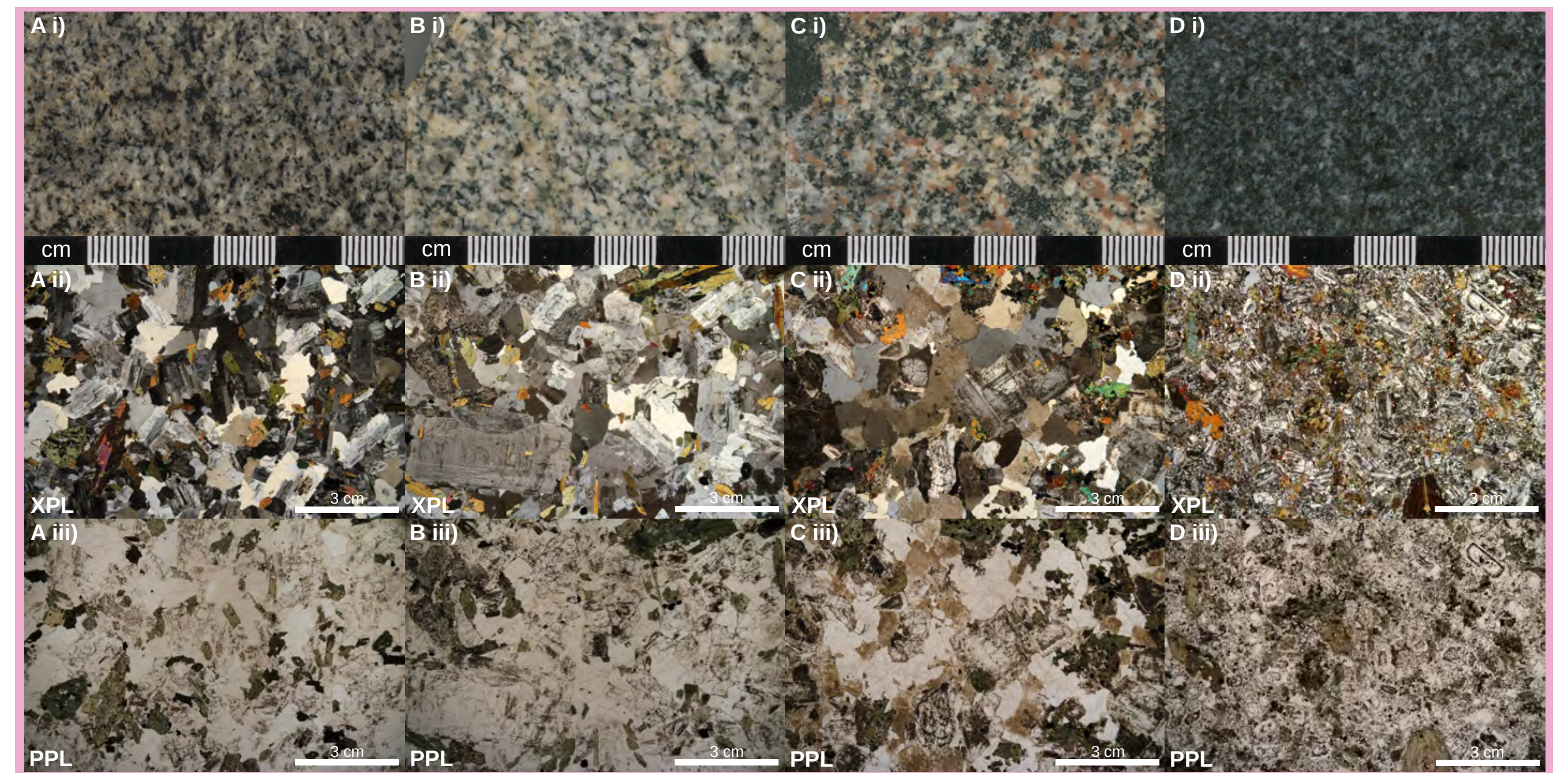

Figure 4. Eastern Magmatic Axis Petrography. **A)** Pennask Batholith, Brenda stock inequigranular granodiorite; **B)** Bromley Batholith inequigranular granodiorite; **C)** Cahill Creek Pluton inequigranular granite; **D)** Hedley stock equigranular diorite. **i)** scanned rock photographs and transmitted light photomicrographs: **ii)** cross polarized light (XPL) and **iii)** plane polarized light (PPL).

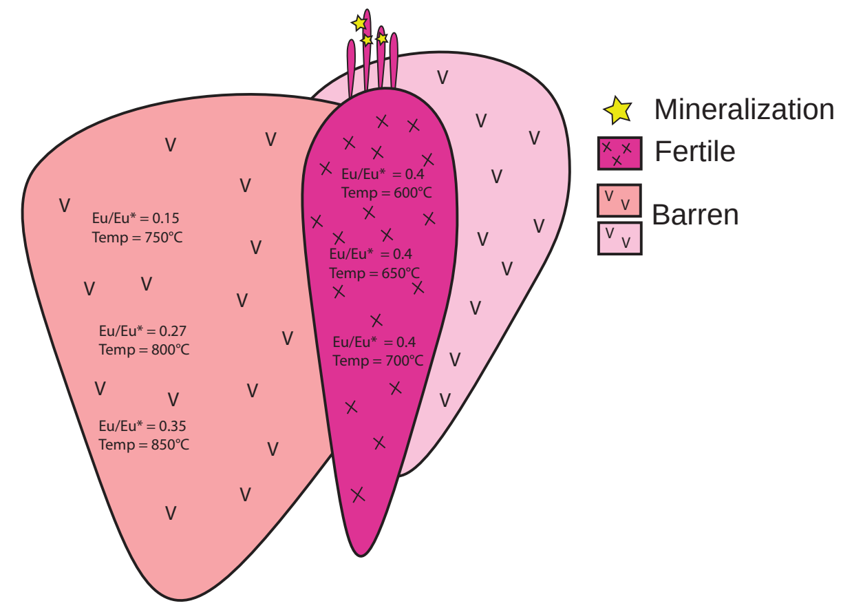

Key Magmatic Parameters (Proxies in Zircon)

1) **Oxidation State** (Eu/Eu* & Ce/Ce*)
2) **Temperature** (Ti-in-zircon-thermometer)
3) **Water Content** (Eu/Eu*)
4) Metal Content
5) Chlorine Content
6) Sulphur Content

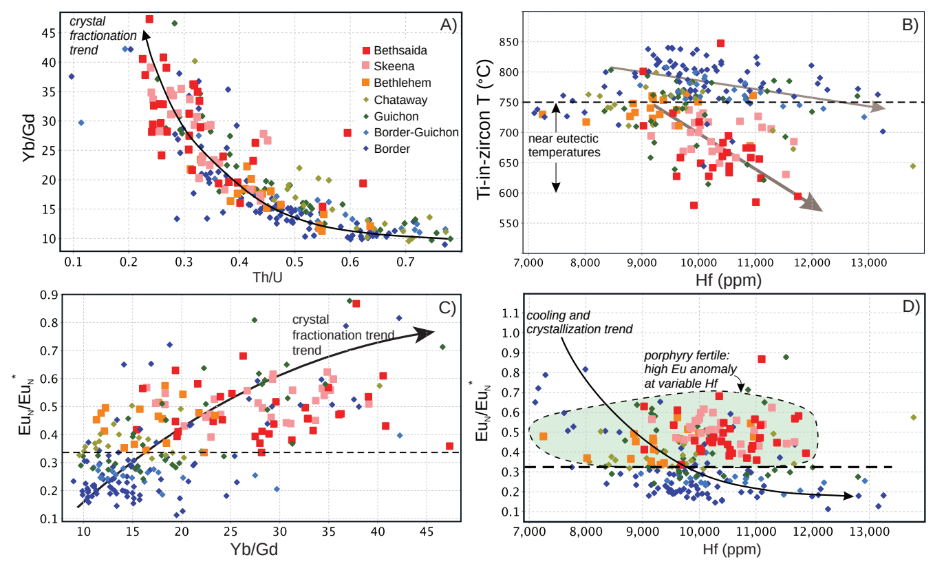

Figure 6. Guichon Creek Batholith zircon trace element scatter plots. Bethsaida, Skeena, and Bethlehem are mineralized intrusions represented by the larger squares; and Chataway, Guichon, Border-Guichon, and Border are unmineralized intrusions represented by the smaller diamonds. A) Th/U vs. Yb/Gd, showing the curved evolution of crystal fractionation. The older unmineralized intrusions are less fractionated than the younger mineralized intrusions. B) Ti-in-zircon temperatures vs. Hf, calculated assuming a melt activity of TiO2 = 0.7, after Ferry and Watson (2007). Mineralized intrusions yield temperatures of 750°C to 600°C, coincident with conditions close to the solidus of hydrous granite, while the unmineralized intrusions yield temperatures of 850°C to 750°C as part of a separate cooling trend. C) Europium anomaly vs. Yb/Gd, as a proxy for apatite and titanite fractionation, showing that the Eu anomalies in the mineralized intrusions are unaffected by crystal fractionation. D) Europium anomaly vs. Hf, showing that the Eu anomaly in the mineralized intrusions are >0.35 regardless of the Hf concentration which is a proxy for cooling and crystallization.

Southern Quesnellia Plutonism

The magmatic axis of Late Triassic to Early Jurassic Quesnellia plutonism migrated episodically eastward, constructing three subparallel linear plutonic axes over an ~36 m.y. period (229–193 Ma; Parrish and Monger, 1992; Kobylinski et al., 2020).

Most Quesnellia porphyry deposits formed between **210 and 195 Ma**, with an especially prolific 6 m.y. long mineralizing event centred at 205 Ma.

As the magmatic axis migrated toward the back arc in the east, plutonic episodes evolved from a **calc-alkaline** affinity to an **alkaline** affinity, and then to **calc-alkaline** to **high-k calc-alkaline**; and porphyry-deposit metal assemblages transitioned from **Cu-Mo** to **Cu-Au** and then to **Cu-Mo±Au**.

Western Magmatic Axis (Late Triassic Calc-alkaline Plutonism)

- Late Triassic (229–206 Ma; D'Angelo et al., 2017; Kobylinski et al., 2020)
- large (up to 1300 km2), thick (>6 km; Ager, 1974)
- composite and zoned, calc-alkaline granodiorite-tonalite suite batholiths
- emplaced 3-7 km deep (Sutherland Brown, 1976)
- host Cu-Mo deposits (6.2 Mt Cu at Highland Valley; 3.0 Mt Cu at Gibraltar)

The zoned batholiths are composed of more mafic dioritic border phases that transition to more felsic granodiorite and tonalite. More mafic phases have up to 45% mafic minerals (hornblende>biotite, minor clinopyroxene and olivine in some batholiths (i.e., Guichon Creek). Felsic phases have as few as 2% mafic minerals, predominantly bio>hb (D'Angelo et al., 2017; Schiarizza, 2015).

The Guichon Creek and Granite Mountain batholiths are the main intrusions that define this magmatic axis; and also host the giant Highland Valley Copper and Gibraltar porphyry Cu districts, respectively. Several other intrusive bodies, such as the Nicola batholith, Alice Lake pluton and other smaller intrusions southeast of the Guichon Creek batholith, make up a contemporaneous but smaller volume subset within the rest of the Western magmatic axis.

Central Magmatic Axis (Late Triassic to Early Jurassic Alkaline Plutonism)

- latest Triassic to Early Jurassic (207–198.6 Ma; Logan and Schiarizza, 2014; Preto et al., 1979)
- smaller (32-120 km2) composite intrusive complexes and batholiths
- compositionally alkaline silica-saturated to -undersaturated, syenite-diorite suite
- shallowly emplaced (~1 km)
- host Au-rich Cu-Au deposits (2.57 Mt Cu and 152.2 t Au at Afton-Ajax; 2.34 Mt Cu and 82.9 t Au at Copper Mountain)

The older intrusive phases in the complexes are often equigranular and the younger intrusions are more often porphyritic, reflecting shallow emplacement depths. Diorites are up to 42% mafics (pyroxene, lesser biotite, and local hornblende). Monzonitic phases typically host 5-20% mafic phases (cpx>bio) in the Copper Mountain intrusive complex and biotite-only in the Iron Mask batholith (Preto, 1972; Logan and Mihalynuk, 2005).

The Mount Polley, Spout Lake and Rayfield River intrusive complexes, Iron Mask batholith and Copper Mountain intrusive complex are the main intrusions that define the Central magmatic axis, which were emplaced in assemblage three and four of the Nicola group (Schiarizza, 2019). The Iron Mask batholith hosts a number of Cu-Au occurrences, most notably the Afton and Ajax deposits; and the Copper Mountain and Mount Polley intrusive complexes each host a porphyry Cu-Au district of the same name. Several smaller alkaline intrusions that make up the rest of the central magmatic axis are east of the larger intrusive bodies that define the central magmatic axis.

Eastern Magmatic Axis (Late Triassic to Early Jurassic Calc-alkaline Plutonism)

- Late Triassic to Early Jurassic (205-192.7 Ma; Calderwood et al., 1990)
- large batholiths (up to 1300 km2), composite and zoned
- calc-alkaline to high-K granodiorite-quartz diorite suite batholiths
- emplaced 3-5 km deep (del Real et al., 2017)
- host Cu-Mo and Cu-Au deposits (0.28 Mt Cu and 0.07 Mt Mo at Brenda and 0.79 Mt Cu inferred at Woodjam)

The composite batholiths usually have older equigranular quartz dioritic intrusions and younger inequigranular granodiorite to monzogranite intrusions. The earlier intrusions are more mafic with 10-25% mafic minerals predominantly consisting of hb>bio, local cpx in the more dioritic phases. Younger intrusions typically have 10-15% mafic minerals consisting of hb>bio in the Takomkane batholith and bio>hb in the Pennask batholith (Soregaroli and Whitford, 1976; Schiarizza et al., 2009).

The Bromley, Pennask, Wild Horse, Thuya and Takomkane batholiths define this magmatic axis. The Pennask and Takomkane batholiths host the past-producing Brenda Cu-Mo mine and Woodjam district, respectfully. This axis also includes several smaller granite to diorite plutons farther east , such as the Cahill Creek pluton and Hedley intrusion, in addition to several smaller, concentrically zoned, Alaskan-type ultramafic bodies that intrude the Nicola Group along the easternmost margins of the axis.

Methods and Sampling

Roadside sampling was conducted in 2018, 2019 and 2020 to collect nine rock, four glacial-till, and three stream-sediment samples that reflect the regional plutonic variability within and between the three magmatic axes of the Late Triassic to Early Jurassic southern Quesnellia arc. These samples will be supplemented with the existing zircon trace-element data on the Guichon Creek, Granite Mountain, and Takomkane batholiths completed by Bouzari et al. (2020), Lee et al. (2020), Lee et al. (in press) and Kobylinski et al. (2020).

Glacial-till and stream-sediment samples were collected to:

1. test the effectiveness of using detrital zircons as an exploration tool;
2. to get broader representation of the Quesnellia arc and its intrusive bodies; and
3. to increase the potential of obtaining zircons from silica-undersaturated to weakly silica-saturated intrusions, such as the Iron Mask batholith and Copper Mountain intrusive complex, that typically have low zircon yields.

Till samples were taken in arid areas with low topographic relief because the streams lack sufficient energy to move clasts and are choked with organic material. Till samples were taken from the banks of small streams or roadcuts using a trowel and were dry sieved to <1 mm in the field. At the Iron Mask batholith, three till samples were taken progressively farther down ice from each other to sample an increased proportion of the Iron Mask intrusive rocks in the till relative to the Nicola Group volcanic rocks that are up ice of the batholith. One glaciofluvial-till sample was collected from down ice of the Pennask batholith.

Stream-sediment samples were taken from areas with sufficient topographic relief and rainfall for running water to erode and transport rock clasts and presumably mineral grains. One stream-sediment sample was collected from a major drainage that is a catchment point downstream of the Pennask batholith and was wet sieved to <1 mm in the stream. Two stream-sediment samples were collected from point bars along the Similkameen River that were currently above the water line progressively further downstream of the Copper Mountain intrusive complex and were brought back to the lab to be dry sieved to < 1 mm.

Future Work

Rock Prep & Zircon Sep: Samples will be crushed, sieved, washed and hand-panned prior to heavy-liquid separation using methylene iodide solution to separate them into heavy and light fractions. Approximately 30–50 zircons will be picked from each rock sample and 100–200 zircons from each stream-sediment and till sample and mounted in an epoxy puck.

Imaging & Classification: Zircons will be imaged in reflected light and cathodoluminescence, and the morphology of the crystals will be classified to identify zircon populations with characteristic habit and growth bands.

Analysis: Appropriate inclusion-free spots will be chosen and analyzed at The University of British Columbia (UBC) Pacific Centre for Isotopic and Geochemical Research (PCIGR) using laser-ablation inductively coupled plasma–mass spectrometry (LA-ICP-MS) to determine the **trace-element composition** as well as the **U-Pb geochronology**. Zircon cores and rims will both be analyzed in each sample when possible. Alkali feldspars will be picked from the light fraction and mounted on a puck to be analyzed for composition and **Pb isotopes** via LA-ICP-MS. A fresh portion of the rock samples will be analyzed for major oxides, trace elements and iron speciation.

After completion of the analytical work, we will:

1. **characterize the magmatic fertility** of each intrusion and batholith;
2. identify evidence of **magmatic processes** such as magma mixing, fractionation, mafic magma recharge, and volatile saturation;
3. attempt to determine how these magmatic processes **influence the formation of porphyry copper deposits**; and
4. determine what **mineral chemistry signatures** in zircon are expressed by these processes.

This then allows consideration of the variability in these magmatic fertility signatures within and between the magmatic axes of the Quesnellia arc while relating this information to the tectonic history and magmatic characteristics of the arc to highlight changes in fertility throughout the evolution of the arc.

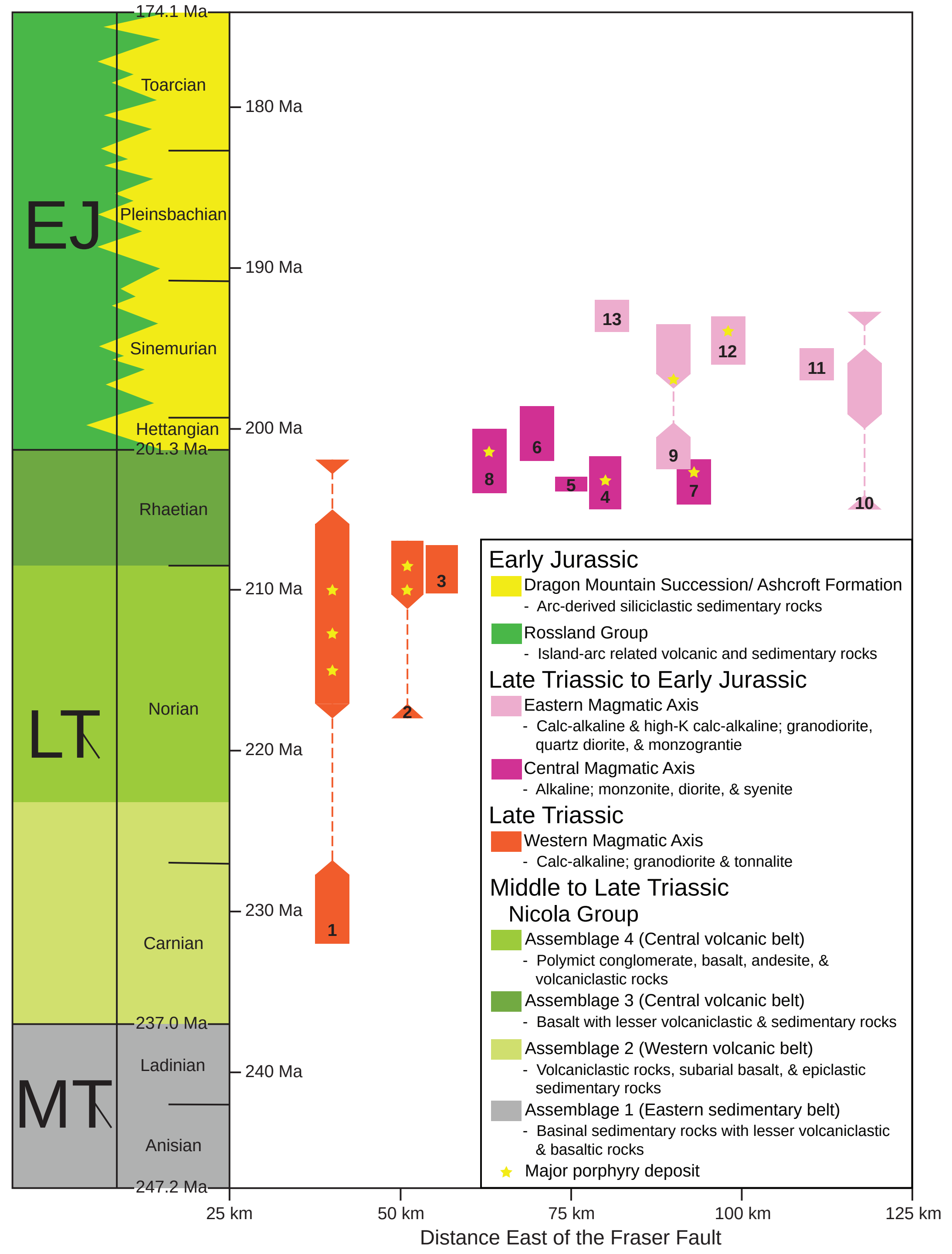

Figure 5. Late Triassic to Early Jurassic plutonic suites and stratigraphy of southern Quesnellia. Numbers and age date reference: 1, Granite Mountain batholith (Kobylinski et al., 2020; Harding et al., 2012); 2, Guichon Creek batholith (D'Angelo et al., 2017; Lee et al., 2020); 3, Alice Lake pluton (Preto et al., 1979); 4, Mount Polley (Mortenson et al., 1995; Logan et al., 2007); 5, Spout Lake pluton (Whitaker et al., 1998; Schiarizza et al., 2009) ; 6, Rayfield River (Logan and Schiarizza, 2014); 7, Iron Mask batholith (Mortenson et al., 1995; Logan and Mihalynuk, 2014); 8, Copper Mountain (Mortenson et al., 1995; Logan et al., 2011); 9, Takomkane batholith (Whitaker et al., 1998; Schiarizza et al., 2009; Logan et al., 2011); 10, Thuya batholith (Schiarizza et al., 2002; Calderwood et al., 1990); 11, Wild Horse batholith (Parrish and Monger, 1992); 12, Pennask batholith (Logan et al., 2011); 13, Bromley batholith (Parrish and Monger, 1992). Solid bars indicate periods of major batholith construction, triangles indicate brief periods of magmatism and dashed lines indicate breaks in magmatism or periods of reduced magmatism. Stars indicate major porphyry deposits with producing mines, except for the star on the Takomkane batholith (9) which is a deposit with an inferred resource. Multiple stars on the Granite Mountain (1) and Guichon Creek batholith (2) indicate distinct periods of mineralization, not the number of deposits. The distance east of the Fraser Fault for the Granite Mountain Batholith (1) and Mount Polley (4) was based on the projection of the fault which does not crop out as far north as these intrusions.

Summary

There is a very strong geological and geochronological framework that documents the changes in the Quesnellia arc throughout time, resulting in varying magma chemistries, emplacement depths, and styles of plutons and associated porphyry mineralization (Mortensen et al., 1995; McMillan et al., 1996; Logan et al., 2011; Logan and Mihalynuk, 2014; Schiarizza, 2014). This provides a foundation upon which investigations of variability in magmatic porphyry fertility throughout arc evolution can be undertaken, in this case by evaluating the chemistry of zircons.

Glacial-till and stream-sediment samples have been taken to test the effectiveness of using detrital zircons as an exploration tool, and as a means to increase the zircon representation of the arc and to increase the potential for obtaining zircons from silica-undersaturated to weakly silica-saturated intrusions that typically have low zircon yields.

The ability to identify fertile arc magmas and understand variability within and between different arc settings will enable explorers to better recognize magmas with the potential to form an economic porphyry Cu deposit and differentiate them from barren intrusions. This research will be applied to develop an exploration toolkit for

Acknowledgments

This project is part of the Mineral Deposit Research Unit's Porphyry Indicator Minerals (PIMS) project. Geoscience BC is thanked for its financial contribution in support of this project in the form of a 2020 Geoscience BC Scholarship. Additional funding was provided by the Society of Economic Geologists Canada.

Research supported by:

Geoscience BC
SEG Canada Foundation
THE UNIVERSITY OF BRITISH COLUMBIA

References

[1] Ager, C.A. (1974): The three-dimensional structure of batholiths as deduced from gravity data; Ph.D. thesis, The University of British Columbia, 143 p., URL <https://doi.org/10.14288/1.0052998> [October 2020].
[2] Bouzari, F., Hart, C.J.R. and Bissig, T. (2020): Assessing British Columbia porphyry fertility in British Columbia batholiths using zircons; Geoscience BC Report 2020-07, MDRU Publication 450, 24 p.
[3] Calderwood, A.R., van der Heyden, P., and Armstrong, R.L. (1990) Geochronometry of the Thuya, Takomkane, Raft and Baldy batholiths, south-central British Columbia; Geological Association of Canada–Mineralogical Association, Annual Meeting, Vancouver, British Columbia, Program with abstracts, v. 15, p. A19.
[4] Colpron, M. and Nelson, J.L. (2020): A digital atlas of terranes for the northern Cordillera; Yukon Geological Survey, URL <http://data.geology.gov.yk.ca/Compilation/2> [October 2020].
[5] Colpron, M. and Price, R.A. (1995): Tectonic significance of the Kootenay terrane, southeastern Canadian Cordillera: an alternative model; Geology, v. 23, p. 25–28, URL <https://doi.org/10.1130/0091-7613(1995)023<0025:TSOTKT>2.3.CO;2> [October 2020].
[6] Cui, Y., Miller, D., Schiarizza, P. and Diakow, L.J. (2017): British Columbia digital geology; BC Ministry of Energy, Mines and Petroleum Resources, BC Geological Survey, Open File 2017-8, 9 p., URL <http://cmscontent.nrs.gov.bc.ca/geoscience/PublicationCatalogue/OpenFile/BCGS_OF2017-08.pdf> [October 2020].
[7] D'Angelo, M., Miguel, A., Hollings, P., Byrne, K., Piercey, S. and Creaser, R. (2017): Petrogenesis and magmatic evolution of the Guichon Creek batholith: Highland Valley porphyry Cu±(Mo) district, south-central British Columbia; Economic Geology, v. 112, p. 1857–1888, URL <https://doi.org/10.5382/econgeo.2017.4532> [October 2020].
[8] del Real, I., Bouzari, F, Rainbow, A., Bissig, T., Blackwell, J, Sherlock, R., Thompson, J.F.H. and Hart, C.J.R. (2017): Spatially and temporally associated porphyry deposits with distinct Cu/Au/Mo ratios, Woodjam district, central British Columbia; Economic Geology, v. 112, p. 1673–1717, URL <https://doi.org/10.5382/econgeo.2017.4526> [October 2020].
[9] Harding, B. (2012): The characterization of molybdenum mineralization at the Gibraltar mines Cu-Mo porphyry, central British Columbia; B.Sc. thesis, Queen's University, 52 p.
[10] Kobylinski, C., Hattori, K., Smith, S. and Plouffe, A. (2020): Protracted magmatism and mineralized hydrothermal activity at the Gibraltar porphyry copper-molybdenum deposit, British Columbia; Economic Geology, v. 115, no. 5, p. 1119–1136, URL <https://doi.org/doi: 10.5382/econgeo.4724> [October 2020].
[11] Lee, R.G., Bryne, K., D'Angelo, M.D., Hart, C.J.R., Hollings, P., Gleeson, S.A. and Alfaro, M. (2020): Using zircon trace element composition to assess porphyry copper potential of the Guichon Creek batholith and Highland Valley Copper deposit, south-central British Columbia; Mineralium Deposita, URL <https://doi.org/10.1007/s00126-020-00961-1> [October 2020].
[12] Lee, R.G., Plouffe, A., Ferbey, T., Hart, C.J.R., Hollings, P. and Gleeson, S.A. (in press): Recognizing porphyry copper potential from till zircon composition: a case study from the Highland Valley porphyry district, south-central British Columbia; Economic Geology Scientific Communications, accepted for publication.
[13] Little, H.W. (1960): Nelson map-area, west half, British Columbia (82F W1/2); Geological Survey of Canada, Memoir 308, 205 p., URL <https://doi.org/10.4095/100535> [October 2020].
[14] Logan, J.M. and Mihalynuk, M.G. (2005): Porphyry Cu-Au deposits of the Iron Mask batholith, southeastern British Columbia; in Geological Fieldwork 2004, BC Ministry of Energy, Mines and Petroleum Resources, BC Geological Survey, Paper 2005-1, p. 249–270, URL <http://cmscontent.nrs.gov.bc.ca/geoscience/PublicationCatalogue/Paper/BCGS_P2005-RR07_Logan.pdf> [October 2020].
[15] Logan, J.M. and Mihalynuk, M.G. (2014): Tectonic controls on Early Mesozoic paired alkaline porphyry deposit belts (Cu-Au ± Ag-Pt-Pd-Mo) within the Canadian Cordillera; Economic Geology, v. 109, p. 827–858, URL <https://doi.org/10.2113/econgeo.109.4.827> [October 2020].
[16] Logan, J.M. and Schiarizza, P. (2014): The Rayfield River pluton, south-central British Columbia (NTS 92P/6): Geologic setting and copper mineralization; in Geological Fieldwork 2013, BC Ministry of Energy, and Mines and Petroleum Resources, BC Geological Survey, Paper 2014-1, p. 15-27, URL <http://cmscontent.nrs.gov.bc.ca/geoscience/PublicationCatalogue/Paper/BCGS_P2014-01-02_Logan.pdf> [January 2021].
[17] Logan, J.M., Mihalynuk, M.G., Friedman, R.M. and Creaser, R.A. (2011): Age constraints of mineralization at the Brenda and Woodjam Cu-Mo+/-Au porphyry deposits – an Early Jurassic calcalkaline event, south-central British Columbia; in Geological Fieldwork 2010, BC Ministry of Energy, Mines and Petroleum Resources, BC Geological Survey, Paper 2011-01, p. 129–144, URL <http://cmscontent.nrs.gov.bc.ca/geoscience/PublicationCatalogue/Paper/BCGS_P2011-01-09_Logan.pdf> [October 2020].
[18] Logan, J.M., Mihalynuk, M.G., Ullrich, T. and Friedman, R.M. (2007): U-Pb ages of intrusive rocks and 40Ar/39Ar plateau ages of copper-gold-silver mineralization associated with alkaline intrusive centres at Mount Polley and the Iron Mask batholith, southern and central British Columbia; in Geological Fieldwork 2006, BC Ministry of Energy, Mines and Petroleum Resources, BC Geological Survey, Paper 2007-1, p. 93–116, URL <http://cmscontent.nrs.gov.bc.ca/geoscience/PublicationCatalogue/Paper/BCGS_P2007-01-10_Logan.pdf> [October 2020].
[19] McMillan, W.J. (1981): Nicola project – Merritt area; BC Ministry of Energy, Mines and Petroleum Resources, BC Geological Survey, Preliminary Map 47 (2 sheets), scale 1:25 000, URL <http://cmscontent.nrs.gov.bc.ca/geoscience/PublicationCatalogue/PreliminaryMap/BCGS_PM47.pdf> [October 2020].
[20] McMillan, W.J., Thompson, J.F.H., Hart, C.J.R. and Johnston, S.T. (1996): Porphyry deposits of the Canadian Cordilleran; Geoscience Canada, v. 23, p. 125–134.
[21] Monger, J.W.H. (1985): Structural evolution of the southwestern Intermontane belt, Ashcroft and Hope map areas, British Columbia; in Current Research, Part A, Geological Survey of Canada, Paper 85-lA, p. 349–3523.
[22] Mortensen, J.K., Ghosh, D.K. and Ferri, F. (1995): U-Pb geochronology of intrusive rocks associated with copper-gold porphyry deposits in the Canadian Cordillera; in Porphyry Deposits of the Northwestern Cordillera of North America, T.G. Schroeter (ed.), Canadian Institute of Mining, Metallurgy and Petroleum, Special Volume 46, p. 142–158.
[23] Mortimer, N. (1987): The Nicola Group: Late Triassic and Early Jurassic subduction-related volcanism in British Columbia; Canadian Journal of Earth Sciences, v. 24, p. 2521–2536, URL <https://doi.org/10.1139/e87-236> [October 2020].
[24] Nixon, G.T., Archibald, D.A. and Heaman, L.M. (1993): 40Ar-39Ar and U-Pb geochronometry of the Polaris Alaskan type complex, British Columbia: precise timing of Quesnellia–North America interaction, Geological Association of Canada–Mineralogical Association of Canada, Joint Annual Meeting, Waterloo, Ontario, Program with Abstracts, p. 76.
[25] Parrish, R.R. and Monger, J.W.H. (1992): New U-Pb dates from southwestern British Columbia; in Radiogenic Age and Isotopic Studies, Report 5, Geological Survey of Canada, p. 87–108.
[26] Preto, V.A. (1972): Geology of Copper Mountain, British Columbia; BC Ministry of Energy, Mines and Petroleum Resources, BC Geological Survey, Bulletin 59, 87 p., URL <http://cmscontent.nrs.gov.bc.ca/geoscience/PublicationCatalogue/Bulletin/BCGS_B059.pdf> [October 2020].
[27] Preto, V.A. (1979): Geology of the Nicola Group between Merritt and Princeton; BC Ministry of Energy, Mines and Petroleum Resources, BC Geological Survey, Bulletin 69, 90 p., URL <http://cmscontent.nrs.gov.bc.ca/geoscience/PublicationCatalogue/Bulletin/BCGS_B069.pdf> [October 2020].
[28] Read, P.B. and Okulitch, A.V. (1977): The Triassic unconformity of south-central British Columbia; Canadian Journal of Earth Sciences, v. 14, p. 606–638, URL <https://doi.org/10.1139/e77-063> [October 2020].
[29] Schiarizza, P. (2014): Geological setting of the Granite Mountain batholith, host to the Gibraltar porphyry Cu-Mo deposit, south-central British Columbia; in Geological Fieldwork 2013, BC Ministry of Energy, Mines and Petroleum Resources, BC Geological Survey, Paper 2014-1, p. 95–110, URL <http://cmscontent.nrs.gov.bc.ca/geoscience/PublicationCatalogue/Paper/BCGS_P2014-01-06_Schiarizza.pdf> [October 2020].
[30] Schiarizza, P. (2015): Geological setting of the Granite Mountain batholith, south-central British Columbia; in Geological Fieldwork 2014, BC Ministry of Energy, Mines and Petroleum Resources, BC Geological Survey, Paper 2015-1, p. 19-39, URL <http://cmscontent.nrs.gov.bc.ca/geoscience/PublicationCatalogue/Paper/BCGS_P2015-01-02_Schiarizza.pdf> [October 2020].
[31] Schiarizza, P. (2016): Toward a regional stratigraphic framework for the Nicola Group: preliminary results from the Bridge Lake–Quesnel River area; in Geological Fieldwork 2015, BC Ministry of Energy, Mines and Petroleum Resources, BC Geological Survey, Paper 2016-1, p. 13–30, URL <http://cmscontent.nrs.gov.bc.ca/geoscience/PublicationCatalogue/Paper/BCGS_P2016-01-02_Schiarizza.pdf> [October 2020].
[32] Schiarizza, P. (2019): Geology of the Nicola Group in the Bridge Lake–Quesnel River area, south-central British Columbia; in Geological Fieldwork 2018, BC Ministry of Energy, Mines and Petroleum Resources, BC Geological Survey, Paper 2019-01, p. 15–30, URL <http://cmscontent.nrs.gov.bc.ca/geoscience/PublicationCatalogue/Paper/BCGS_P2019-01-02_Schiarizza.pdf> [October 2020].
[33] Schiarizza, P., Bell, K. and Bayliss, S. (2009): Geology and mineral occurrences of the Murphy Lake area, south-central British Columbia (NTS 93A/03); in Geological Fieldwork 2013, BC Ministry of Energy, Mines and Petroleum Resources, BC Geological Survey, Paper 2014-1, p. 95–110, URL <http://cmscontent.nrs.gov.bc.ca/geoscience/PublicationCatalogue/Paper/BCGS_P2009-01-15_Schiarizza.pdf> [October 2020].
[34] Soregaroli, A.E. and Whitford, D.F. (1976): Brenda; in Porphyry Deposits of the Canadian Cordillera, A. Sutherland Brown (ed.), Canadian Institute of Mining and Metallurgy, Special Volume 15, p. 186–194.
[35] Sutherland Brown, A., editor (1976): Porphyry deposits of the Canadian Cordillera; Canadian Institute of Mining, Metallurgy and Petroleum, Special Volume 15, 510 p.
[36] Travers, W.B. (1978): Overturned Nicola and Ashcroft strata and their relations to the Cache Creek Group, southwestern Intermontane belt, British Columbia; Canadian Journal of Earth Sciences, v. 15, p. 99–116, URL <https://doi.org/10.1139/e78-009> [October 2020].
[37] Whiteaker, R.J., Mortensen, J.K. and Friedman, R.M. (1998): U-Pb geochronology, Pb isotopic signatures and geochemistry of an Early Jurassic alkalic porphyry system near Lac La Hache; in Geological Fieldwork 1997, BC Ministry of Energy, Mines and Petroleum Resources, BC Geological Survey, Paper 1998-01, p. 33-1–33-14.